

## A MIRROR MOUNT FOR CRYOGENIC ENVIRONMENTS

Bijan Iraninejad and Daniel Vukobratovich  
Optical Sciences Center  
University of Arizona  
Tucson, AZ 85721

Ralph M. Richard  
Department of Civil Engineering  
University of Arizona

and Ramsey K. Melugin  
NASA Ames Research Center

### Abstract

The finite element method was used to study the effect of mount-induced aberrations on the optical surface of a lightweight double arch mirror subjected to cryogenic temperatures.

The mount design was controlled by the requirements imposed on the optical surface quality and stress levels. The finite element analysis was used to define the feasible range of mount parameters and the selection of a design within the feasible region. The final design consisted of three spring-loaded Invar T-clamps that uniquely define the location of the mirror, three radially compliant parallel spring guides that remove the effect of radial contraction of structure in cryogenic temperatures, and a flexible baseplate that was used to reduce the effect of temperature-induced baseplate tilt errors. The experimental results from the application of this system to an existing 20-inch fused silica double arch mirror are shown, and possible improvements in system performance are discussed.

### Introduction

To fully utilize the low background environment, the shuttle infrared telescope facility will be operated at temperatures of about 10°K. The purpose of this study was to design a mounting mechanism that could be used to provide transition between the primary mirror and the telescope structure at cryogenic temperatures. In addition to maintaining the optical alignment and a good surface quality, the mount must be designed to neither exceed the microyield stress level during launch nor to reach the yield stress in emergency landing.

The mount was specifically designed for a 20-in.-diameter fused-silica double arch mirror (Fig. 1). In this study, the forces and/or moments transferred from the mount to the mirror due to cryogenic temperatures, gravity loading, and various mount errors, as well as the magnitude of stress under the above conditions were calculated analytically. The analytical results were then used in conjunction with the finite element techniques to establish the mirror surface quality under different conditions. By using the magnitude of stress in the mount and figure quality of the mirror as the basic criteria, a range of acceptable design dimensions for the mount was found and an optimum design was designated.

### Design concept

In the proposed design, the mirror is supported by three clamp and flexure assemblies. The flexures are radially compliant, but stiff in all other directions. These flexures allow the aluminum mirror cell to expand or contract relative to the mirror, yet uniquely determine the mirror's position (Fig. 1).

The mirror clamp consists of a T-shaped Invar 36 member that goes into a similarly shaped socket in the back of the mirror. The mirror socket contacts the clamp only along a conical surface with a 70° inclination angle. The clamp is preloaded by a Belleville spring washer and is pinned in place.

The clamps are attached to flexures that are in turn attached to the mirror cell. These flexures are stiff in the axial and tangential directions but are compliant in the radial direction. By using three flexures, each with its radial compliance at 120° to the others, the mirror's position is uniquely determined without overconstraint. The radial compliance allows contraction of the mirror cell relative to the mirror while inducing a minimum figure or alignment change.

The flexures take the form of parallel spring guides. In comparison with a single blade flexure, a parallel spring guide offers greater stiffness and a higher fundamental frequency and does not transmit any moment to the glass.

The chosen flexure material, titanium 6Al-4V ELI, allows the greatest compliance at cryogenic temperature without becoming excessively brittle. The titanium alloy has a relatively small change in size when cooled and is corrosion resistant.

The mirror cell is a 0.95-cm-thick (3/8 in.) aluminum plate with three supports at 120°; the flexures are mounted to the base plate with a 60° phase angle with respect to the cell supports.

**Design requirements**

The final figure quality of the mirror in operation is directly affected by the flexure design. As shown in Fig. 1, a parallel guide flexure is defined by five parameters. However, a study of the parameters showed that for typical flexure dimensions, the design is very insensitive to variation in T, the thickness of the top and bottom plate. Therefore, the design space was reduced to four dimensions.

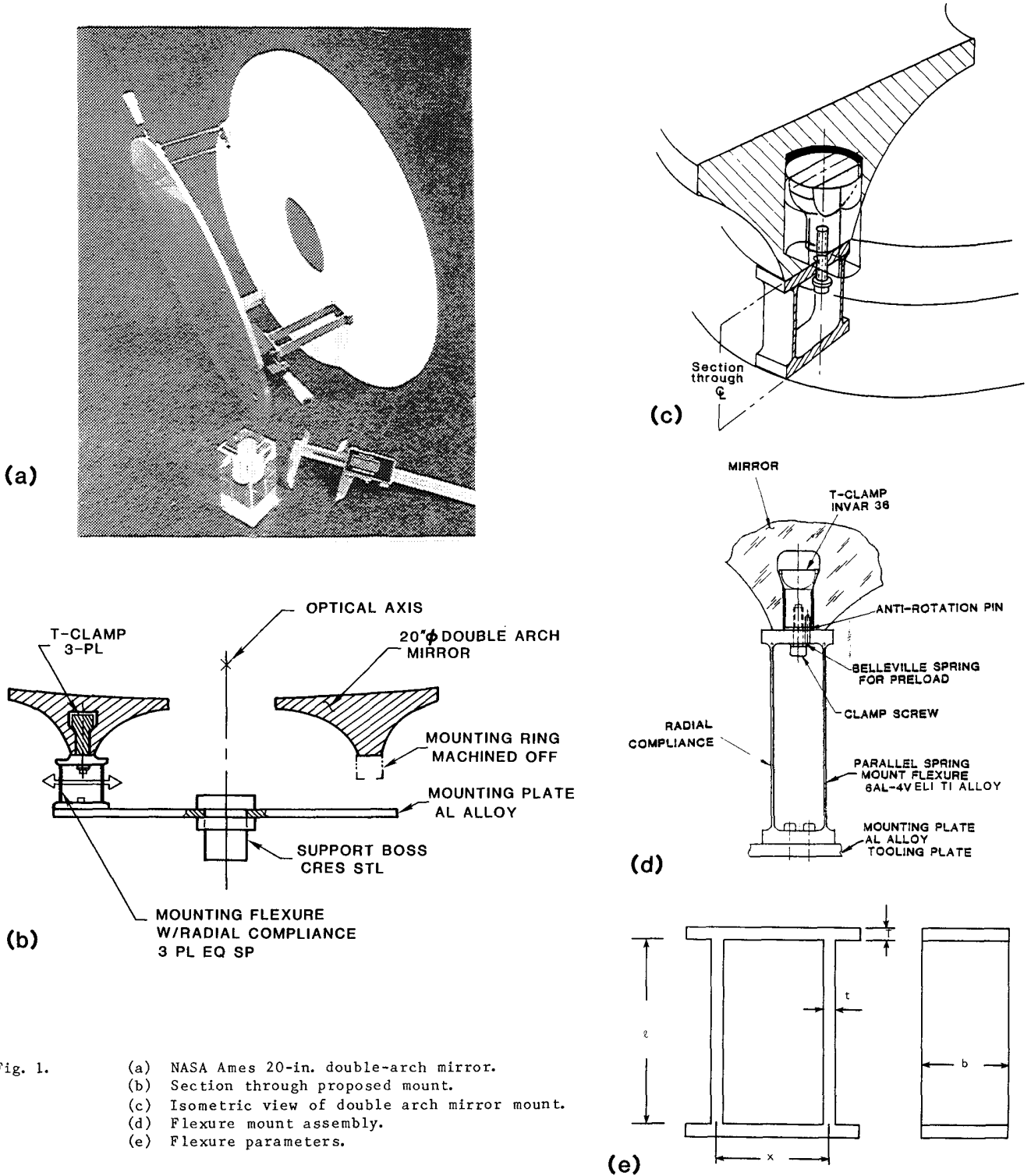


Fig. 1. (a) NASA Ames 20-in. double-arch mirror. (b) Section through proposed mount. (c) Isometric view of double arch mirror mount. (d) Flexure mount assembly. (e) Flexure parameters.

Based on the dimensional limitations imposed on the design by the manufacturing process and the space requirements, the design parameters were constrained to a feasible region given in Table 1-a.

Establishing estimates of possible mount or temperature-induced errors is possible only in a statistical sense. Instead of imposing performance requirements on the overall surface quality, we limited the contribution of independent sources of figure deterioration. Furthermore, the surface quality was quantified by the root mean square (RMS) value of the differences between the deformed mirror surface and the undeformed surface measured at 644 regularly spaced grid points. In doing so, it is assumed that tilt and focus terms can be corrected by the telescope system. The surface quality requirements imposed on the design are shown in Table 1-b.

The maximum stress in the flexures was designed not to exceed the microyield limit, either in operation or during launch. However, for an emergency landing, stresses as high as the yield point were allowed. A safety factor of 2 was used. The stress requirements are shown in Table 1-c.

Table 1. Design Requirements

(a) Manufacturing/Space Requirements

Minimum size (inch)		Maximum size (inch)
0.03	Blade thickness	0.04
2.00	Flexure height	4.00
0.60	Blade separation	2.00
0.40	Flexure width	2.00

(c) Stress Requirements

Stress source	Maximum normal stress (psi)
During operation	57,500
During launch	57,500
During emergency landing	120,000

(b) Surface quality requirements

Error sources	Maximum RMS error (10 <sup>-6</sup> in.)
Differential contraction	1.0
Localized radial tilt	2.5
Localized tangential tilt	2.5
Flexure non-parallelism	2.5

Analysis

To calculate the forces transferred from the flexures to the mirror and the internal stresses developed in flexures, the mirror was assumed to be infinitely stiff. By using this assumption, which leads to conservative results, the size of the finite element model and the number of runs necessary to perform the analysis was substantially reduced.

Besides the flexures, the mirror cell plays an important role in reducing the effect of mount errors on the figure quality. For example, a localized tilt in a flexible mirror cell induces negligible moment in a stiff flexure, however, as the cell becomes stiffer, the moment increases. In other words, a localized tilt in the cell, which can easily develop in a cryogenic environment, is partially transferred to the flexure and partially com-

pensated for in the cell itself. To take this interaction into account, the forces and stresses in the flexures due to temperature errors in the cell should be multiplied by a reduction factor, R

$$R = \frac{f_f}{f_f + f_c}, \quad (1)$$

where  $f_f$  and  $f_c$  are the flexibility of flexure and the cell in a given direction, respectively.

The figure error during operation is determined by several factors including the differential contraction between the mirror and its cell, the temperature-induced localized tilts in the cell, and the mount manufacturing errors. The net effect of the above factors on the mirror is to induce a set of forces and moments to the mirror through flexures. Clearly, the surface deformation depends on the magnitude and direction of the applied forces and moments. Therefore, analytical expressions for calculating the loads induced by flexures were formulated.

Exploring the feasible design region and examining all the loading conditions for each feasible design, if possible, would have required a considerable number of finite element runs; therefore, an alternative approach was used. First, the various loading conditions encountered by the mirror were resolved to their most basic components. Then, the sensitivity of the mirror surface was established in terms of Zernike coefficients and

RMS surface error using the finite element method for each basic loading component. Once the sensitivity functions were calculated, the optical performance of the surface for the various flexure designs and loading conditions were determined by a simple combination of the proper proportions of the basic loading components.

By using the above approach, it became possible to use a simple summation equation:

$$Z = \sum_{i=1}^k c_i a_{n,i}^m R_n^m \quad (2)$$

where:

$R_n^m$  = Zernike polynomial term  
 $a_{n,i}^m$  = Zernike coefficient (sensitivity function) for the  $i$ th loading component  
 $c_i$  = magnitude of sensitivity coefficient for the  $i$ th loading component  
 $Z$  = deformed surface

to define the deformed surface for any flexure design without making a separate finite element run. Furthermore, the above equation provides an implicit and continuous definition of the surface over the feasible design region. Analytical expressions were used to determine the stress in the flexures for a given geometry and loading.

It would have been ideal to optimize the design for minimum RMS in the mirror and minimum stress in the flexures. However, these two objectives are in direct conflict. Therefore, the stress requirements were treated as constraints and several attempts were made to optimize the design for a minimum RMS. The optimization package used was OPTLIB. Unfortunately, the optimization techniques used failed to approach the global optimum; and therefore, in the absence of a better approach, a parametric study of the feasible design region was performed. As a result of this study, a flexure design 91 mm high (3.6 in.) and 15 mm wide (0.60 in.) with a blade thickness of 1 mm (0.04 in.) and blade separation of 25 mm (1.00 in.) was selected. As shown in Table 2, the above design satisfies all the imposed requirements (compare Table 1 and 2). Obviously, the actual figure error observed during operation will differ from that of Table 2 due to the random presence of mount errors. An example of the mirror surface for a given mount error is shown in Fig. 2.

To gain insight into the stress distribution in the mirror due to the clamping force, an axisymmetric model was built. The stress contours for the principal stress in a section going through the socket is shown in Fig. 3(a). Generally speaking, the magnitude of both tension and compression stress in the mirror, does not exceed 600 psi.

Table 2. Optical and structural performance of the proposed design.

	RMS in. x 10 <sup>6</sup>	Normal stress (psi)	
		Without mount error	With mount error
Operation	0.049	7,150	24,097
Launch	---	10,392	42,098
Emergency landing	---	58,456	93,242
Localized radial tilt*	0.763	717	---
Localized tangential tilt*	2.062	2,826	---
Nonparallelism error**	0.075	13,407	---

\*0.001 radian localized tilt

\*\*0.001 inch nonparallelism between the two blades

### Experiment

The mount design was built and tested (Fig. 3(b)). To simulate a cryogenic soak at -423°F, precision adjustable slides were used to radially move the flexure bases. The tests were performed using a Shack interferometer. Unfortunately, the measured results were of the same order of magnitude as the limits of accuracy of the testing and data reduction procedures used. Therefore, the test results cannot be used for a direct comparison with analysis. However, the test results are consistent with analysis and show that the effect of cryogenic soak on a mirror is within the imposed requirements. Obviously, to gain a better understanding of the effect of low temperatures on the mirror, a true cryogenic test is needed.

Contour size Width Page size -M- -N- -P- -Q-  
 0.300 0.500 2.000 -0.450 -0.150 0.150 0.450



Residual wavefront variations over uniform mesh

RTS	RMS	Max	Min	Span	Volume
664.0	2.324	5.980	-6.336	12.316	18.698

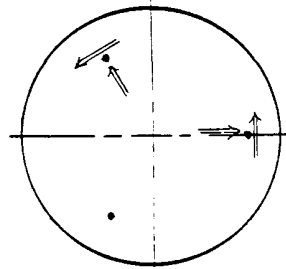


Fig. 2. The effect of cool down and radial and tangential tilt in two flexure locations on the mirror figure. Units =  $10^{-6}$  in.

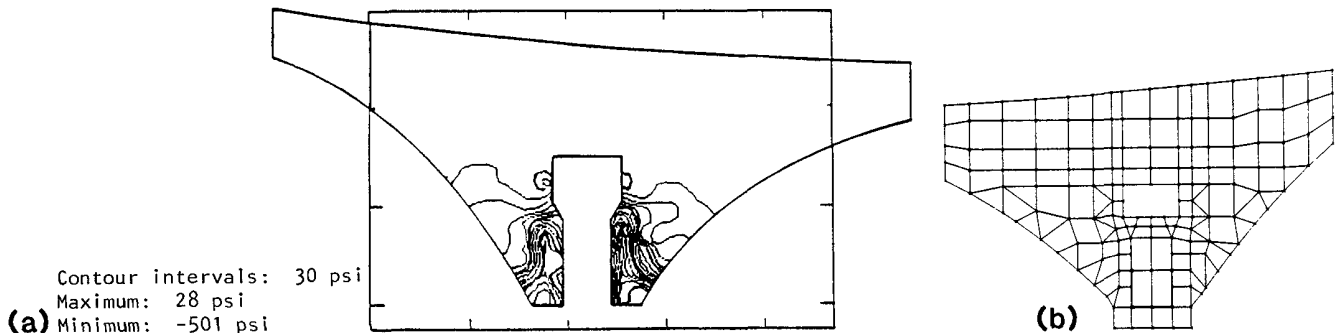


Fig. 3(a). Stress profile of the principal normal stress for a clamping force equal to the weight of the mirror. (b). The axisymmetric finite element model.

### References

1. Vukobratovich, D., et al., "Optimum shapes for lightweighted mirrors," Proc. SPIE 332, 1982.
2. Schwartzberg, F. R., et al, "Cryogenic materials data handbook," AFML. TDR. **280**, National Technical Information Service, 1970.
3. Gabriele, G. A., and K. M. Ragsdell, "OPTLIB: An optimization program library," Purdue Research Foundation, 1979.
4. Bathe, K. J., et al., "SAP IV, A structural analysis program for static and dynamic response of linear systems," University of California at Berkely, 1974.